REVISTA DE LA
ASOCIACIÓN GEOLÓGICA
ARGENTINA
www.geologica.org.ar
Marzo 2025

The basal friction in the modeling of the propagation of shallow landslides – debris flow using r.avaflow

Johnnatan PALACIO[1*], Martin MERGILI[2], Edier ARISTIZÁBAL[3] and Oscar ECHEVERRI[1]

[1] Departamento de Ingeniería civil, Universidad Nacional de Colombia, Medellín, Colombia.

[2] University of Graz, Institute of Geography and Regional Science, Graz, Austria.

[3] Departamento de Geociencias, Universidad Nacional de Colombia, Colombia, Medellín, Colombia.

(*) E-mail: japalacioc@unal.edu.co

Editor: Ricardo A. Astini

Recibido: 22/10/2024

Aceptado: 26/05/2025

ABSTRACT

Landslides pose a significant natural hazard around the world and rainfall is the primary triggering factor in Colombia. Many investigations focus on the occurrence of landslides, and the areas affected by their propagation (runout) should also be considered. Landslide runout is influenced by different variables such as cohesion, variable density, erosion, and entrainment, where basal friction plays an important role. This investigation focuses on the influence of basal friction variation in modelling of shallow landslides using r.avaflow. The model is implemented in the municipality of Mocoa located in Colombian southwestern. Where 3 hours of heavy rainfall triggered a clustered shallow landslides and chain processes on March 31st, 2017. The event caused 306 lives lost. Some results from modeling shallow landslides – debris flow under or overestimate the affected areas according to basal friction used. However, analysis indicates that basal friction equal to the internal friction of the material has better results. As well, results indicate that the minimum heights estimated ranging from 0.51 m to 0.61 m offer conservative results to perform zoning of the possible affected areas.

Keywords: Cluster; hazard; modeling; runout; debris flow.

RESUMEN

La fricción basal en la modelización de la propagación de deslizamientos en masa superficiales -flujos de detritos- utilizando r.avaflow. Los movimientos en masa representan una seria amenaza de origen natural alrededor del mundo, en Colombia el principal detonante de estos son las lluvias. Muchas investigaciones se centran en la ocurrencia de movimientos en masa, y también se deben considerar las áreas afectadas por su propagación. La propagación de movimientos en masa está influenciada por diferentes variables como la cohesión, la densidad, la erosión y el arrastre, donde la fricción basal juega un papel importante. Esta investigación se centra en la influencia de la variación de la fricción basal en el modelado de la propagación de movimientos en masa poco profundos utilizando la herramienta r.avaflow, implementada en el suroccidente colombiano en el municipio de Mocoa. El evento analizado corresponde al ocurrido el 31 de marzo del 2017. En la zona, cerca de 3 horas de lluvia desencadenaron un conjunto de movimientos en masa superficiales y procesos en cadena, causando aproximadamente 306 muertes. Los resultados, arrojan que en algunos casos se subestiman o sobreestiman las áreas afectadas de acuerdo con la fricción basal utilizada. Sin embargo, los análisis indican que una fricción basal igual a la fricción interna del material presenta mejores resultados. Asimismo, indican que las alturas mínimas estimadas para considerar una afectación oscilan entre 0.51 m y 0.61 m. Además, se consideran como resultados conservadores y adecuados para realizar zonificaciones de posibles áreas afectadas.

Palabras clave: Enjambre; deslizamiento; amenaza, propagación, flujo de detritos.

INTRODUCTION

Landslides are one of the most destructive natural hazards around the world, causing thousands of deaths, injuries, and damages each year (Petley 2012, Froude and Petley 2018, Dilley et al. 2005, Schuster and Highland 2001, Kjekstad and Highland 2009, Schuster and Highland 2003, Dai et al. 2002, Kirschbaum et al. 2009). Rainfall, earthquakes, volcanic activity, and anthropical activity are factors that can cause them. However, rainfall is the primary triggering factor in tropical and high mountain settings such as the Colombian Andes (Froude and Petley 2018, Gómez et al. 2023).

The occurrence of landslides in the country is common due to two environmental factors, especially in the central zone known as the Andean region. (i) Mountains and steep slopes cover one-third of the country as the result of the subduction of the Nazca Plate beneath the South American Plate along the western margin. (ii) The central zone has seasonal rains from March to May and September to November. Which, during the cold phase of the El Niño/Southern Oscillation (La Niña) become more frequent and stronger (Poveda 2004), so landslides occurrences increase. Aristizábal and Sánchez (2019) estimates that rains caused 87 % of the landslides that occurred in the country between 1900 – 2018, and the Andean region contributes about 93 % of all landslides occurred.

Gómez et al. (2023) reports that Colombia has the highest number of landslides in the world that caused 1 to 10 deaths, totaling approximately 1600 landslides in the total years reviewed. Besides, landslide frequency of 10 per 1000 km^2. Landslides, according to Cruden and Varnes (1996), encompass a broad range of mass movements, and their classification is based on material – rock, earth, or debris – and movement type (flow, topple, fall, slide, or spread). Landslides triggered by rainfall are typically translational slide types, with – shallow – thicknesses not exceeding 3 m (Moser and Hohensinn 1983, Engelen 1967, Campbell 1974, Anderson and Sitar 1995). Shallow landslides usually occur on steep slopes with a planar or slightly undulating failure surface, controlled primarily by joints, discontinuities, or in the interface with materials with less permeability (Varnes 1978). The updated classification by Hungr et al. (2014) illustrates, how following failure, a shallow slide can evolve into more rapid movements such as flows or avalanches depending on water content, material, entrainment, and topography. According to recent records, debris flows have caused some of the most severe damage to the inhabitants and infrastructure, such as occurred in Tarazá (2007), Salgar (2015), Mocoa (2017) and Dabeiba (2020). Many of them happened because of the occurrence of clustered shallow landslides, tens to hundreds of landslides were triggered by intense and/or prolonged rainfalls in a short period (hours) in a defined area. Some landslides were deposited in drainages and contributed sediments to the formation of more damaging events in chain processes.

Many investigations focus on the occurrence of landslides, and the areas affected by their propagation should also be considered. There are several approaches for analyzing landslide mass propagation (runout). They can be mainly grouped into (i) empirical-statistical methods, based mainly on geometric estimations of volume, area, height difference, length, and travel angle (Hungr et al. 2005). (ii) analytical methods, which neglect the internal deformation, and the mass is reduced to a point representing of the center of mass (Dai et al. 2002, Quan Luna et al. 2012). (iii) Numerical methods that include discontinuum models that represent the mass by a group of particles and continuum models, as the physical models that, which model in major detail the composition and mobilization mass (Pastor et al. 2014). Many of these methods are applied based on available data, i.e., empirical methods require basic information such as source location (point or area) and topography of the terrain to determine the potential travel distance and area of deposition. While physically based models require additional detailed information as unstable mass composition, geotechnical parameters, and volume.

Landslide runout is influenced by different variables and parameters, including acceleration, velocity, terrain, material composition, internal deformation, saturation degree, rheological settings, and basal friction. Deepen in the rheology, the mixture of soil, vegetation and/or debris with a certain degree of saturation does not behave as a Newtonian fluid after failure. The mass propagates with internal deformation and no linear behavior. This mixture sometimes also has some cohesion, and variable density, and in most cases loses and gains material according to the rate of erosion and entrainment, where basal friction plays an important role. Pudasaini and Krautblatter (2021) contrast between erosion and entrainment. Erosion is described as the procedure of loose material separating from the bed surface, whereas entrainment is defined as the incorporation of the removed material into the mass being mobilized. These two phenomena are significant in the propagation of landslides, specifically in the increase of mass or volume and destructive potential. This research focuses on the analysis of propagation of shallow landslide – debris flow triggered by rainfall in Mocoa (2017), considering the influence of basal friction variation in modelling using the r.avaflow tool that incorporates several physics-based models and phase interaction. We use single phase analysis since the velocity change between phases is negligible. The basic geotechnical parameter required is the internal friction of the materials, which is the starting point to establish the range of values for the basal friction. In this research, it's ranging from 80 % to 100 % of the internal friction. In each basin, the modeling corresponds to a 5 % increase in the defined range. The validation criteria reflect the value of the basal friction, i.e., the proportion of internal friction with which the best results were produced. In addition to the minimum flow height for zoning the areas affected by shallow landslide propagation.

STUDY AREA

Mocoa is in the Colombian southwestern, it is the capital of the department of Putumayo. It has 683 km^2 of rural and 580 km^2 of urban area. The study area covers 30.5 km^2. It includes the basins of the Mulato River, Sangoyaco River and Taruca Creek. These tributaries of Mocoa River flow mainly in a W-E direction from the eastern mountain range, where the maximum elevation of the study area is 2344 m a.s.l., and slopes close to 79° to plains located at 550 m a.s.l. They flow into the Mocoa River in the urban area of the municipality (Figure 1). Therefore, in terms of natural hazards such as debris flows, especially in concatenated events, these tributaries are the most influential.

Geological settings

Mocoa occupies two completely different environments. To the west, it is located on the eastern Colombian mountain range. To the east, it is in the Amazonian foothills. As a result, it has geomorphological and geological diversity. From a geomorphological point of view there are steep terrains and steep V-shaped valleys in the west and fans, terraces, and plains to the east. There is a system of faults crossing the study area in a N-S, NE-SW direction. The Mulato, Campucama, Mocoa - La Tebaida and Cantayaco faults and the lineaments of the Taruca Creek and the Sangoyaco River are in (SGC 2017b).

The most important faults are Mocoa - La Tebaida and Cantayaco. These structurally divide the study area into 3 zones. According to SGC (2017b, 2018b) the zones can be described as: (i) It is a high slope zone that represents the transition between the eastern mountain range and the Amazonian foothills, bounded by the Mocoa - La Tebaida fault. In this zone, the Mocoa monzogranite outcrops (igneous unit), which in turn is divided into a series of subunits of highly fractured rocks of intermediate quality in the west to very low quality in the east, with residual soils up to 2 m thick. (ii) The middle zone is formed by a sequence of sedimentary rocks of the Pepino and Orito Group formations, which overlay the Rumiyaco Formation. The zone is bounded by the Mocoa - La Tebaida and Cantayaco faults. The Orito Group develops

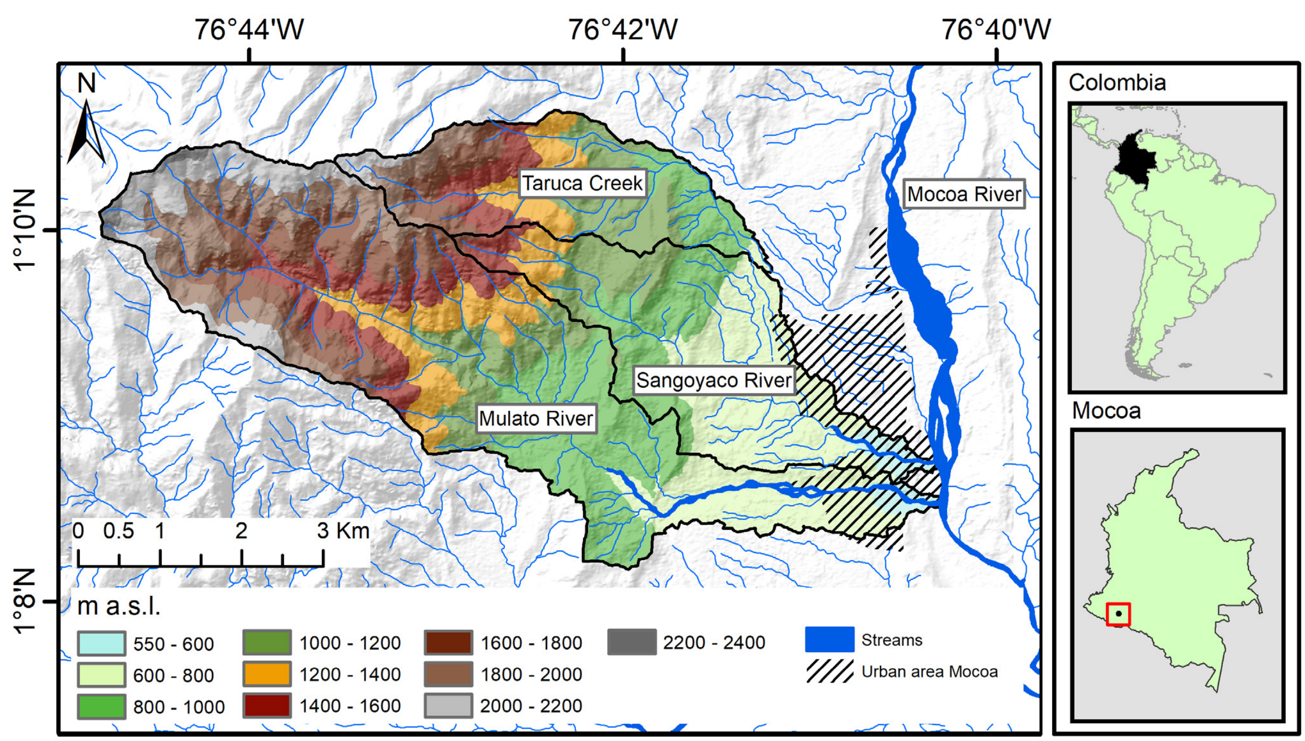

Figure 1. Study area location

soils up to 1.5 m thick in mudstone and siltstone beds. The Pepino Formation is dominated by weathering resistant conglomerates that develop sandy soils in their upper member. (iii) In the Amazonian foothills, the Rumiyaco Formation rises above the Villeta Formation due to the Cantayaco fault and develops soils up to 1.5 m thick, which are generally covered by deposits and terraces of the Mocoa River and its tributaries (Figure 2a).

Debris flow records

Mocoa urban area is located on several fans, including the alluvial fan of Taruca Creek, which extends around 15 km² SGC (2018a). Between 1947 and 2018, there were approximately 15 significant natural hazards that included floods, debris flows, mudflows, and landslides. Table 1 highlights the occurrences related to debris flows that have impacted the urban area, with the occurrence of landslides that produced damming and/or contributed sediments to the event. In 1960, there was an event on Taruca Creek, it had a slight impact on the area where the urban area is now located. Due to the low occupancy at the time, the loss of life and damage was minor. It impacted an area of about 30 ha, whereas the deposits from the 2017 event covered about 50 ha in the same location (SGC 2017a).

Table 1. Historical records of cascade events related to rainfall-triggered landslides in Mocoa. Modified from SGC (2017c)

Type	Year	Basin	Observations
Debris flow	1947	Mulato River	Landslides and damming
Mud flow and debris flow	1960	Taruca Creek	Pre-event 2017
Debris flow	1995	Taruca Creek	Landslides and damming
Debris flow	1998	Mulato, Sangoyaco and Mocoa rivers	Landslides and prolonged rainfalls
Debris flow	2014	Taruca Creek	Landslides
Mud flow and debris flow	2017	*	Landslides
Debris flow	2018	**	Landslides

*Taruca, El Carmen and San Antonio Creek - Mulato, Sangoyaco and Mocoa rivers

**Taruca Creek - lower basin of Mulato and Sangoyaco rivers (Medina Bello et al. 2018)

Climate

Mocoa has a humid warm climate with an average temperature of ~ 23°C, and it does not have a well-defined

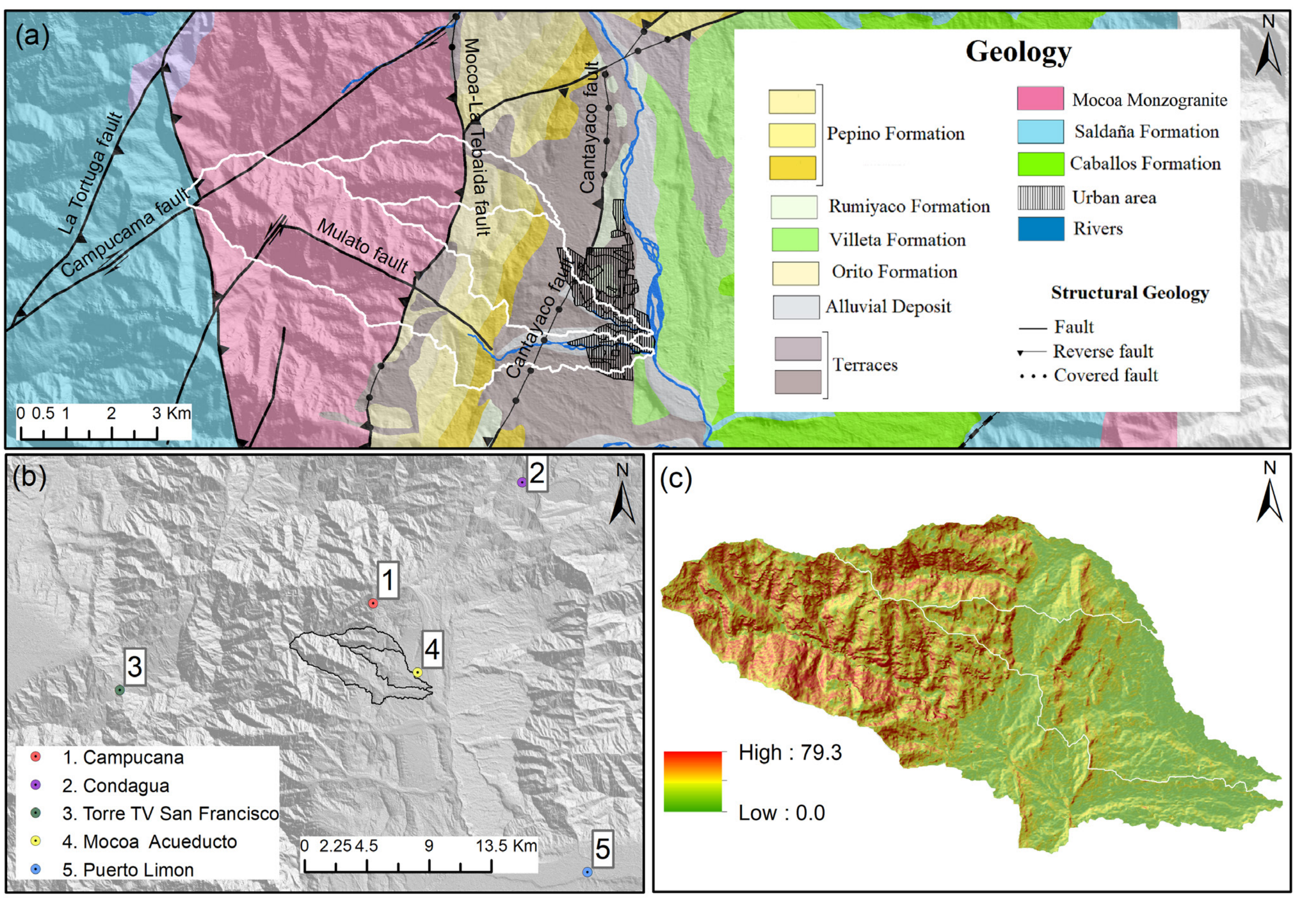

Figure 2. a) Geological setting modified from Núñez Tello (2003), b) nearby pluviometric stations, and c) slope (degrees), to the west there are high slopes corresponding to the Andes high mountain range, while to the east low slopes are found in the Amazonian foothill.

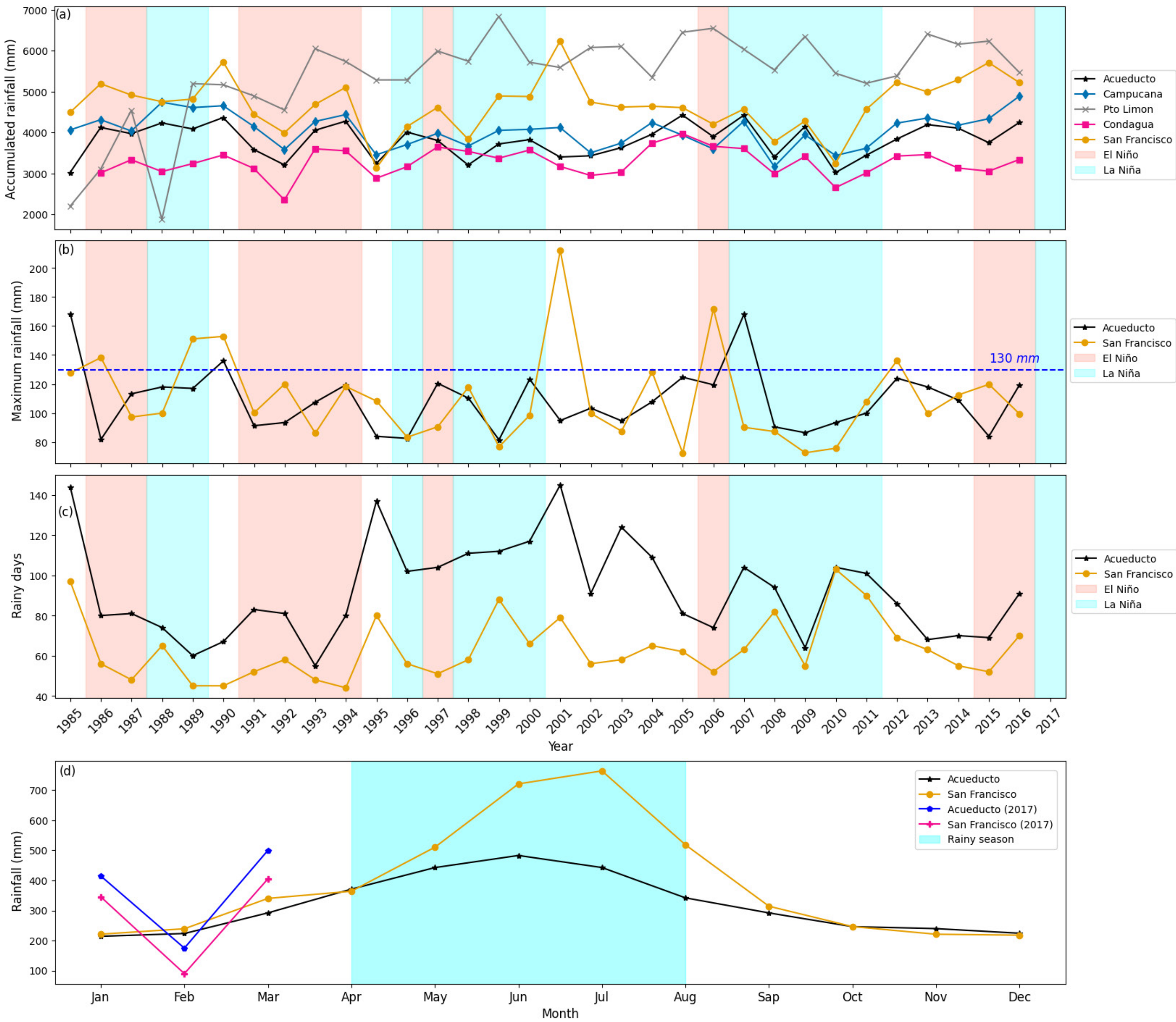

Figure 3. a) Multiannual rainfall distribution from nearby pluviometric stations. b) Maximum multiannual daily rainfall, highlighting the triggering rainfall amount of 130 mm. c) Multiannual rainy days. d) Monthly multiannual rainfall distribution showing rainy season. Figures a), b), and c) show ENSO seasons (*El niño – La niña*). Modified from SGC (2018a). Data provided by IDEAM

dry season. Rainfall occurs throughout the year, with the heaviest rainy season occurring between April and August, with a maximum number of rainy days in May, June, and July (www.ideam.gov.co). The Institute of Hydrology, Meteorology, and Environmental Studies (IDEAM, by its Spanish acronym) has several pluviometric stations in the area, two of them represent the geoenvironmental differences at study area. The San Francisco station represents the climatic conditions of the upper zone of the study basins on the eastern mountain range at an altitude of 3000 m a.s.l., while the Acueducto station is in the urban area representing the conditions of the lower zone in the Amazonian foothills at 650 m a.s.l., the horizontal distance between stations is ~ 21.6 km (2b).

The San Francisco station has an average accumulated rainfall record of 4673.7 mm during a multiannual period between 1985 and 2016, the Acueducto station registered 3813.1 mm. During the rainy season, the monthly multiannual records reveal that San Francisco station had more accumulated rainfall, which indicates heavier rains in fewer days, and nonuniform rainfall distribution in the study zone (Figure 3).

31ST MARCH 2017 DEBRIS FLOW

The night of March 31st and early April 1st (2017), hours of rain triggered hundreds of landslides clustered and chain processes over urban area and surrounding countryside places. According to the National Institute of Legal Medicine and Forensic Sciences, approximately 306 dead people were identified. News reported 322 dead, approximately 330 people injured and, more than 100 people missing (RCN Radio, 2017). The propagation of the largest possesses, such as debris flow, caused the most damage to the population and infrastructure (Figure 4). Slopes between 0° and 25° predominate in the study area; however, the occurrence of landslides is concentrated between 20° and 40°, in convex-convex areas and smaller concave-concave areas. Figure 4 depicts landslides distribution and debris flow damage area. Rainfall triggered ~ 276 landslides, 90 % of them were classified as a debris flow (SGC, 2017c).

The contribution in the Sangoyaco River basin was estimated to be 76940 m3 of solids; in the Mulato River 34009 m3; and in Taruca Creek, 187831 m3 (SGC 2017c). According to Prada-Sarmiento et al. (2019), the materials deposited, studied, and tested by SGC (2017c, 2018a, 2017a, b, 2018b) indicate that the chain processes formed were a debris flow along Taruca Creek (Figure 5). Which was then converted into a hyper-concentrated flow in the Sangoyaco River and a mud flow in the Mulato River.

Triggering rainfall

Records of Acueducto station on March 31st show light rainfall at, 20:00h with peak precipitation at 23:00h of 62.8 mm. At 1:00h on April 1st chain processes impacted the urban area of the municipality Mocoa. Registered accumulated rainfall was ~ 130 mm in three hours, it has been exceeded 3 and 6 times according to Acueducto and San Francisco stations respectively (Figure 3b). SGC (2018b) indicates that this precipitation corresponds to a return period of 5 – 10 years for the Acueducto station and 5 years for the San Francisco station. On the other hand, the accumulated rainfall 38 days before the event for Acueducto station was 600 mm and is repeated more than once a year. However, this accumulated rainfall linked to 130 mm precipitation represents a condition with a return period of 25 years (SGC 2017c). Figure 3d shows multiannual mean monthly precipitation. In March 2017 pluviometric record exceeds 2016 record.

DATA AND METHODS

Landslide propagation estimation is a difficult task, clustered shallow landslides data provide the occurrence and propagation of numerous individual landslides, this information builds up a useful inventory of landslides that occur in similar conditions in a defined area. For modeling, authors have developed models based generally on empirical, analytical, and physical methodologies. The latter is who requires more detailed information. This research employs a physics-based numerical tool r.avaflow, this requires basic inputs such as the digital terrain model (DTM), height of the source areas (volume), spatial distribution of the internal friction of the materials, and basal friction. The DTM is derived from a 5 m spatial resolution GEOSAR image processed and adjusted by SGC (2017c) for investigations of the event occurred on March 31st in Mocoa.

The inventory of ~ 276 landslides (source areas) were carried out by SGC (2017c). However, this research considers 233 landslides – not reactivated – detonated during the March

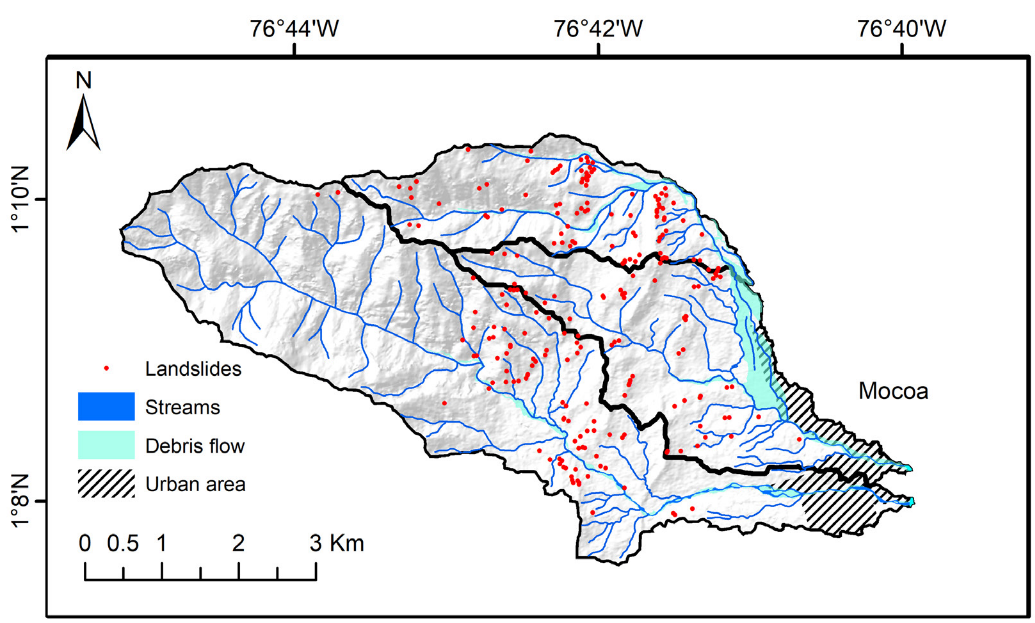

Figure 4. Landslides distribution and debris flow impacted area.

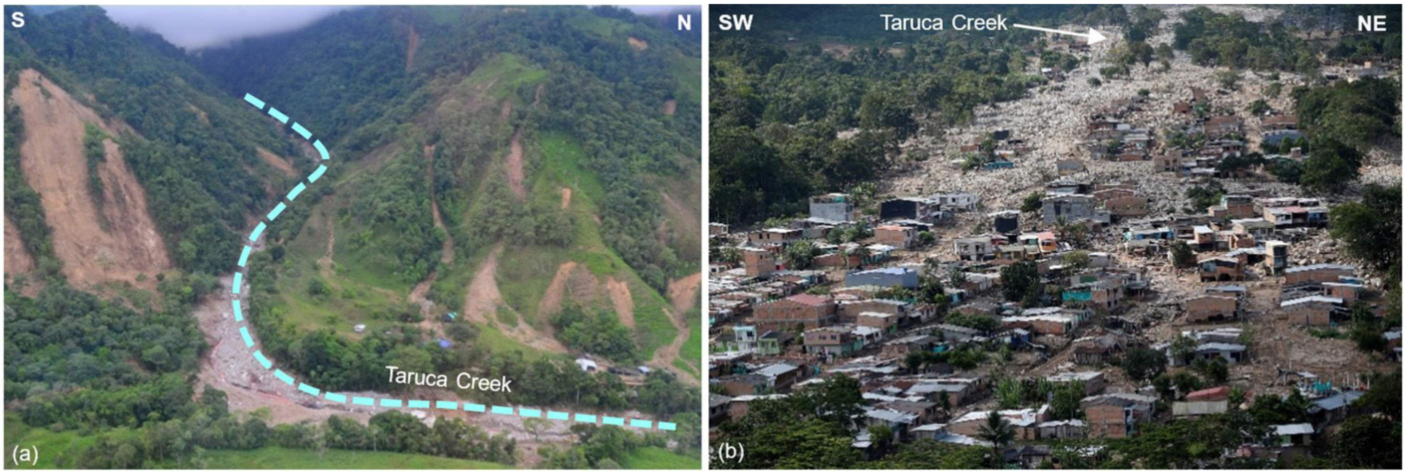

Figure 5. a) Landslides triggered in the Taruca Creek basin. b) Urban area impacted because of debris flow. From Corpoamazonia (https://www.corpoamazonia.gov.co/).

31st event. The geotechnical information comes from studies carried out by the SGC at a scale of 1:25000. The follows sections explains (i) the detail the theoretical foundations and requirements for modeling with the r.avaflow. (ii) establish the parameters for modeling and (iii) presents the validation metrics used. Latest sections present the results and discuss.

r.avaflow

r.avaflow is an open-source computational tool developed as a raster module in GRASS GIS to simulate mass flows and complex process chains. The model computes the propagation from previous defined masses, release masses are input to the model as heights in raster map and/or hydrographs, which are then simulated over the terrain from source area up to deposition zone. Depending on the basic information given and the type of analysis executed, the tool produces different results. It provides hydrographs, ROC plots, 3D animation, height, velocity, pressure of the flow, and other raster maps. The first version of r.avaflow (2017) considers the mixture solid-fluid model of Pudasaini (2012). This study uses r.avaflow 2.3 version, it is feasible for single-phase and multi-phase modeling, it considers the interaction between phases in a redistribution of mass and momentum using a numerical scheme of Wang et al. (2004) linked to dynamic flow model of Pudasaini and Mergili (2019). Recent versions include changes in the basal topography, deposition, dispersion, and phase transformations. Follows are described as the phases considered by Pudasaini and Mergili (2019).

The fluid phase is a mixture of water and very fine particles ranging from colloids to silt, which can be represented using a fluid shear-rate-dependent viscoplastic rheology; the material can behave like a common viscous fluid if the particle concentration is zero.The fine-solid phase is a fine granular material composed of bigger clay particles up to fine gravels, and it is governed by shear- and pressure-dependent Coulomb-viscoplastic rheology, where particle interaction influences energy dissipation.

The solid phase considers coarse material modeling by shear-rate-independent Mohr-Coulomb plastic rheology. With frictional, no viscous behavior.

3-Dimensional three-phase mass flow model is given by balance for mass (eq.1 to eq. 3) and momentum (eq.4 to eq 6) conservation differential equations for the solid, fine-solid, and fluid phases respectively. Where solid, fine-solid, and fluid phases are denoted by the suffix s, fs, and f , respectively. ρ is density, δ the basal friction angle, and Ø the internal friction angle in solid and fine-solid phase and n viscosity is considered in fluid phase.

$$\frac{\partial \alpha_s}{\partial t} + \nabla \cdot (\alpha_s \boldsymbol{u}_s) = 0 \qquad (1)$$

$$\frac{\partial \alpha_{fs}}{\partial t} + \nabla \cdot (\alpha_{fs} \boldsymbol{u}_{fs}) = 0 \qquad (2)$$

$$\frac{\partial \alpha_f}{\partial t} + \nabla \cdot (\alpha_f \boldsymbol{u}_f) = 0 \qquad (3)$$

$$\frac{\partial}{\partial t}(\alpha_s \rho_s \boldsymbol{u}_s) + \nabla \cdot (\alpha_s \rho_s \boldsymbol{u}_s \otimes \boldsymbol{u}_s) = \alpha_s \rho_s \mathbf{f} - \nabla \cdot \alpha_s \boldsymbol{T}_s + p_s \nabla \alpha_s + \boldsymbol{C}_{DG}^{s,f} + \boldsymbol{C}_{DG}^{s,fs} + \boldsymbol{C}_{vm}^{s,f} + \boldsymbol{C}_{vm}^{s,fs} \qquad (4)$$

$$\frac{\partial}{\partial t}(\alpha_{fs} \rho_{fs} \boldsymbol{u}_{fs}) + \nabla \cdot (\alpha_{fs} \rho_{fs} \boldsymbol{u}_{fs} \otimes \boldsymbol{u}_{fs})$$

$$= \alpha_{fs} \rho_{fs} \mathbf{f} - \alpha_{fs} \nabla p_{fs} + \nabla \cdot \alpha_{fs} \tau_{fs} - \boldsymbol{C}_{DG}^{s,fs} + \boldsymbol{C}_{DG}^{fs,f} - \boldsymbol{C}_{vm}^{s,fs} + \boldsymbol{C}_{vm}^{fs,f} \qquad (5)$$

$$\frac{\partial}{\partial t}(\alpha_f \rho_f \boldsymbol{u}_f) + \nabla \cdot (\alpha_f \rho_f \boldsymbol{u}_f \otimes \boldsymbol{u}_f)$$

$$= \alpha_f \rho_f \mathbf{f} - \alpha_f \nabla p_f + \nabla \cdot \alpha_f \tau_f - \boldsymbol{C}_{DG}^{s,f} - \boldsymbol{C}_{DG}^{fs,f} - \boldsymbol{C}_{vm}^{s,f} - \boldsymbol{C}_{vm}^{fs,f} \qquad (6)$$

Where u=(u,v,w) denote the velocities along the flow directions (x,y,z), and α volume fractions with $\alpha_{fs}+\alpha_s+\alpha_f=1$. C_{DG} and C_{vm} constitute the interfacial force densities, the drags and the virtual mass forces respectively. ***T*** is the negative Cauchy stress tensor, τ is the extra stress, and p the pressure. The complete mathematical and physic framework is explained by Pudasaini and Mergili (2019).

Modeling parameters

The simulations are computed considering a solid one-phase model. Although the mass is saturated to some degree, the flow of water within it is minimal, as are the changes in acceleration (Pastor et al, 2014, Tayyebi et al. 2022). So, the contact between the solid and fluid phases is insignificant, and the motion is the same, where the rheology of the solid phase prevails.

r.avaflow being a physically based tool demands detailed information. However, the input data for a single-phase analysis – solid – are minimal. The main input is the volume, considering the soil thickness from the source areas identified at the field (< 2.5 m); shown in Figure 6. The parameters utilized in the modeling are shown in Table 2.

Basal friction describes the contact between the propagating mass and the ground surface and corresponds to the variation of the internal friction of the material in 5% increments from 80 % to 100 % of the internal friction, shown in Figure 6. Spatially every zone is characterized by an angle of internal friction, r.avaflow specifies that the basal friction cannot be higher than the internal friction and in case the user increases it to a higher value, both frictions will be set equal to the given value. For this reason, the modeling is performed considering a basal friction range of 0.8 to 1.0 of the internal friction.

Table 2. Parameters used to modeling in r.avaflow

Symbol	Parameter	Value	Unit
ρ_s	Solid material density (grain density)	2700	kg m^{-3}
ρ_f	Fluid density	1000	kg m^{-3}
Ø	Internal friction angle	Figure 6	Degree
δ	Basal friction angle	0.8 Ø - 1.0 Ø	Degree

Validation metrics

The best-fit parameters can be assessed using validation metrics to explore and analyze the results obtained concerning the existing inventory. Fawcett (2005) proposes four variables, considering model prediction and actual inventory observations. Applied to this study, they can be defined as a set of four scenarios, as follows. True Positive (TP) observed areas that were correctly identified as impacted in the simulation; True Negative (TN) non-impact areas that were correctly identified as non-impacted in the simulation; False Positive (FP) non-impacted area at was incorrectly identified as impacted; False Negative (FN) impacted area that was incorrectly identified as non-impacted. Since both the inventory and the results show an imbalance between impacted and non-impacted areas, with TN exceeding TP. The validation metrics selected do not take TN value into account. If this variable is included, for this specific case the metric would be more a measure of effectiveness of the model by estimating the non-impacted areas rather than the impacted ones. As a result, measures unaffected by the TN were selected (Table 3).

The Factor of Conservativeness (FoC) denotes how conservative the results obtained are, FoC< 1 means that the results are not conservative, while FoC> 1, indicates that they are conservative, and FoC= 1 is the optimal. The predictive accuracy of positive cases is measured by recall or True Positive rate (TPr). Precision, also known as Predictive Positive Value (PPV), is the percentage of impacted areas

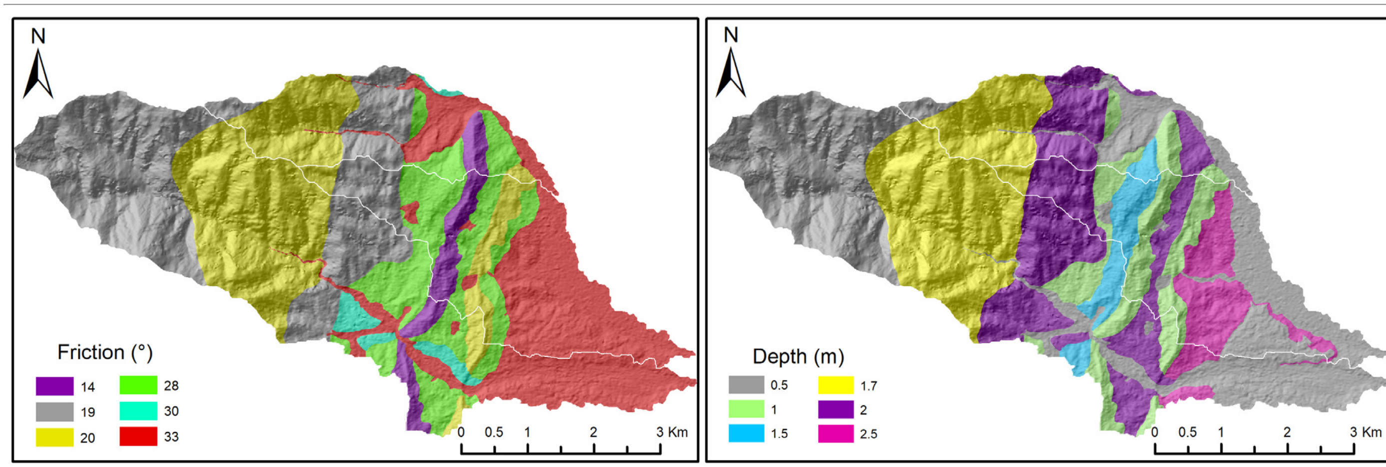

Figure 6. a) Internal friction angle (degrees) and depth (m) distribution (SGC 2017c).

Table 3. Validation criteria

Parameter	Definition	Range	Optimum
Factor of Conservativeness (FoC)	(TP+FP)/ (TP+FN)	[0, ∞]	1.0
F1-Score	2*(PPV+TPr)/ (PPV*TPr)	[0, 1]	1.0
Recall (TPr)	TP/(TP+FN)	[0, 1]	1.0
Precision (PPV)	TP/(TP+FP)	[0, 1]	1.0
TPr: True positive rate PPV: Positive predictive value			
TP: True positive FP: False positive FN: False negative			

relating to the total number of positives identified. The F1-Score combines precision and recall as an accuracy metric.

RESULTS

The results provided by r.avaflow correspond to the height of the flow deposit for each basal friction value in every basin, following the simulation of propagation within a 300 second interval. The Figure 7 illustrates the variation of TPr and F1-Score relating to FoC for each basal friction that is proportionate to the internal friction. When the FoC approaches one, assuming that the basal friction equals the internal friction (δ = 1.00 Ø) yields the most accurate model results. As FoC increases, F1-Score decrease, while TPr rises, showing a loss of accuracy in the positive predictions due to an increase of FP.

Simulations with δ = 1.00 Ø, which produced the highest metrics, are summarized in Table 4, and the metrics for the various minimum – cut-off – flow heights and FoC are presented. In general, the flow height with the best F1-Score in the three basins is close to FoC~ 2. In addition, a similar cut-off flow height from 0.51 m to 0.61 m is observed, differing by 0.1 m between them. In second place are the heights associated with FoC~ 3 and the optimal value for FoC~ 1 is in third place with a cut-off flow height greater than 1 m. For all cases, the lowest F1-Score corresponds to the most conservative results, FoC~ 6.

Figures 8, 9 and 10 show the result achieved considering δ = 1.00 Ø. Each subfigure depicts the area covered by the deposit with the minimum height from which the area of affectation is considered, with increases in the FoC of approximately one. In general, as the FoC increases, the area covered by the deposit increases too since the minimum height considered decreases. So, conservative values of FoC indicate a very low flow height cut-off, from which the affectation will occur, reflecting deposits with more area, whereas non-conservative values have higher minimum flow height cutoffs, representing deposits with less area. Figure 8 presents the results for the Mulato River basin. Figure 8a shows the area covered by the depositional area associated with the optimum FoC~ 1, considering a minimum deposition height of 1.48 m up to a maximum of 10.24 m; some impacted areas (inventory) are not covered due to a relatively high minimum flow height of 1.48 m. However, in Figure 8g, a more conservative result not only covers the impacted areas but also significantly increases it, with a minimum flow height of 0.05 m, thus increasing the FP. For Taruca Creek the result is shown in Figure 9. Figure 9a shows how the deposit areas are minor in the targeted zone concerning the inventoried ones, with a minimum cut-off height of 1.06 m. For FoC~ 2 a larger area is covered and although visually it is not representative; it is more accurate than the results for FoC> 2 as this cover too many areas that were not impacted.

The results for the Sangoyaco River basin (Figure 10) reveal similarities in the areas covered by zthe deposits associated with FoC> 2, which are elongated deposits that differ little from the most conservative result with a minimum flow height of 0.10 m. Although the result linked with the FoC~ 1 fits the impacted areas, it does not cover all of them.

DISCUSSION AND CONCLUDING REMARKS

r.avaflow is a tool based on physical models, the approaches to landslide runout modeling struggle to incorporate material

Table 4. Cut-off flow height and metrics variation for δ=1.00 Ø

Basin	Cut-off flow height (m)	Recall	FoC	F1-Score
Mulato δ=1.00 Ø	1.48	0.35	0.99	0.35
	0.51	0.57	2.10	0.37
	0.26	0.71	3.13	0.34
	0.15	0.78	3.95	0.31
	0.10	0.84	4.83	0.29
	0.05	0.91	6.55	0.24
Taruca δ=1.00 Ø	1.06	0.27	0.97	0.28
	0.61	0.47	2.02	0.31
	0.35	0.63	3.15	0.30
	0.20	0.72	4.26	0.28
	0.15	0.77	4.88	0.26
	0.10	0.83	5.89	0.24
Sangoyaco δ=1.00 Ø	1.03	0.30	0.91	0.31
	0.51	0.51	1.98	0.34
	0.31	0.63	2.99	0.32
	0.21	0.74	3.98	0.30
	0.15	0.81	4.82	0.28
	0.10	0.89	6.18	0.25

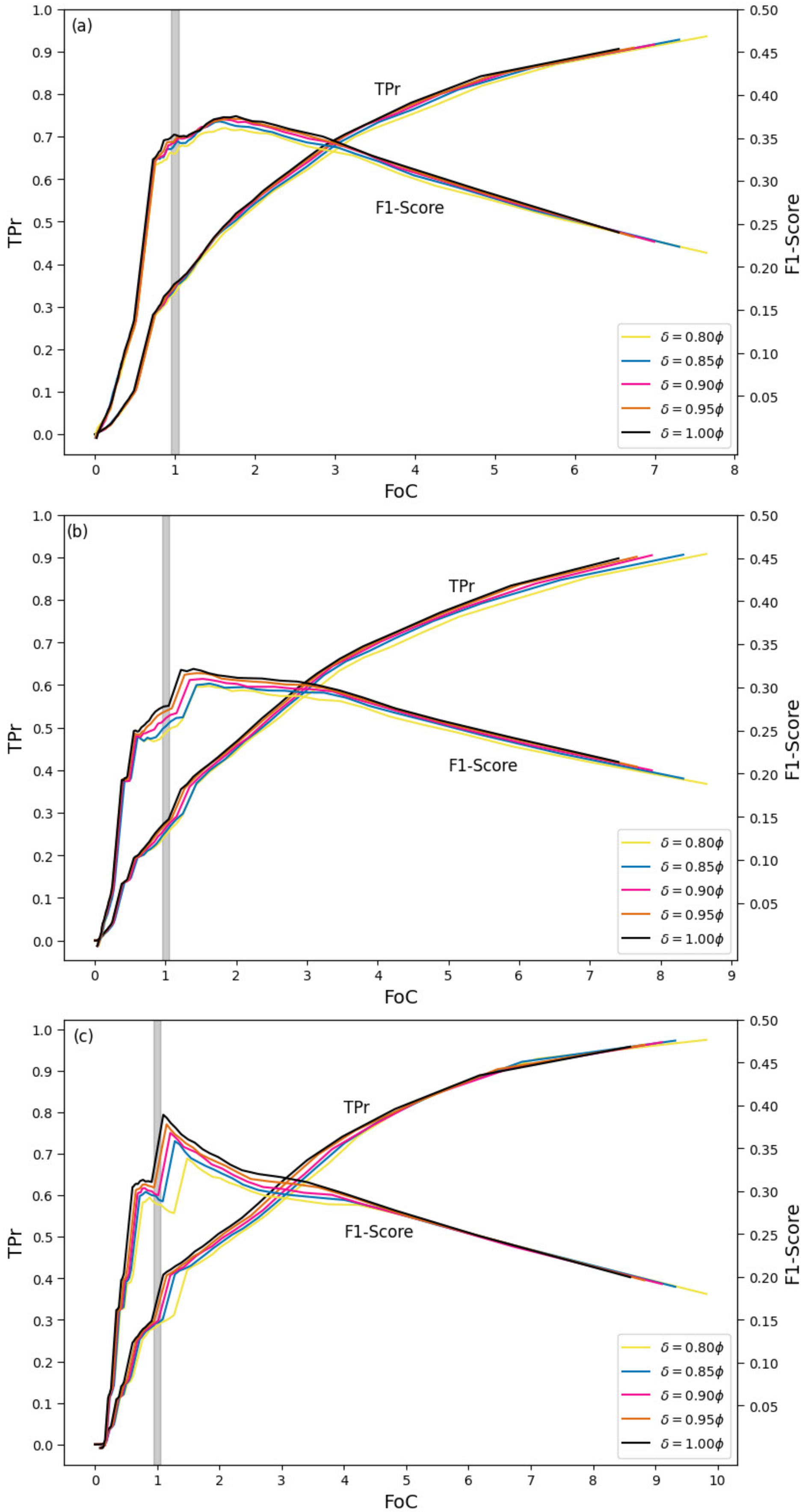

Figure 7. Variation of TPr and F1-Score depending on FoC for each basal friction. a) Mulato River, b) Taruca Creek and c) Sangoyaco River.

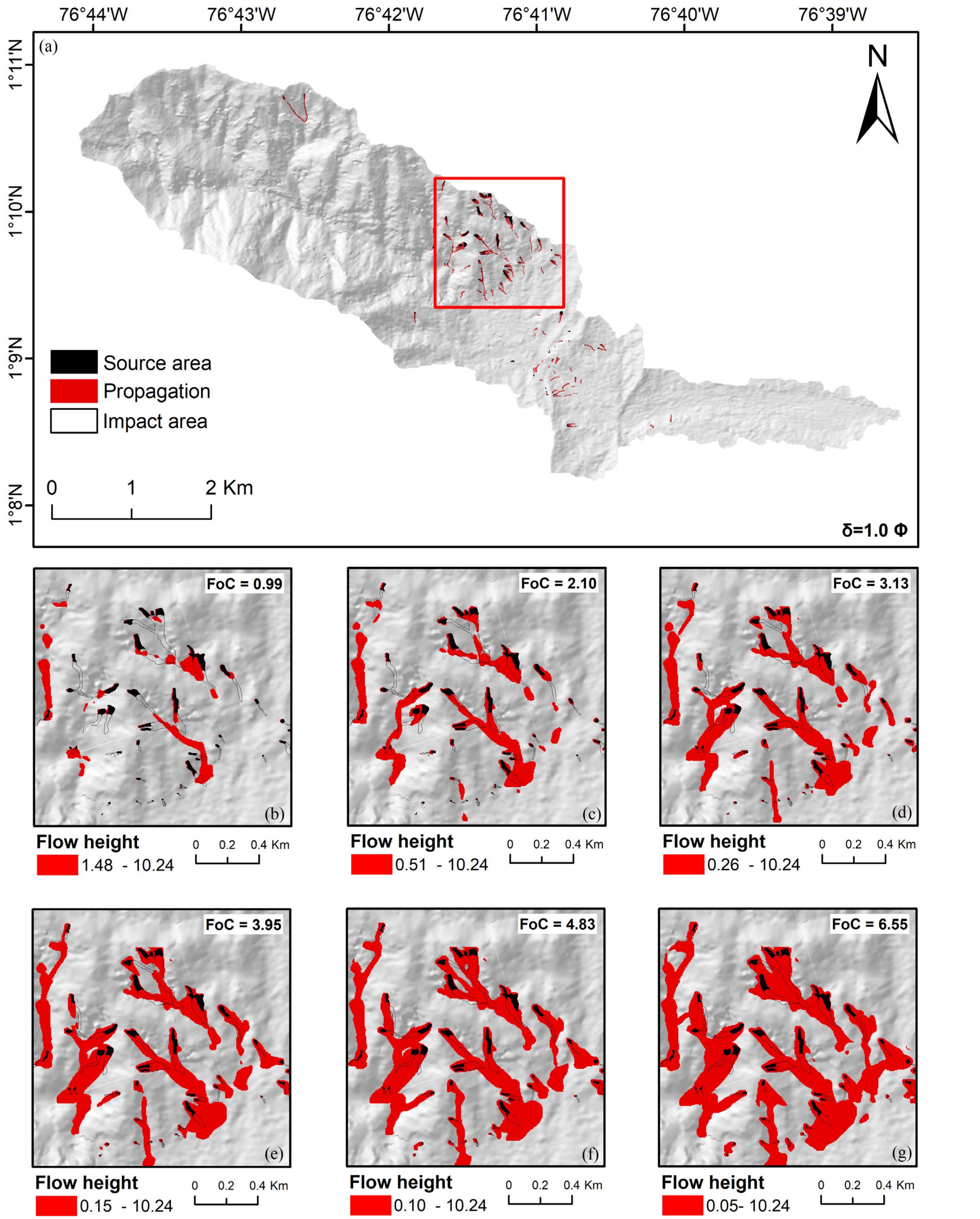

Figure 8. Modeling FoC and flow height (m) - Mulato River.

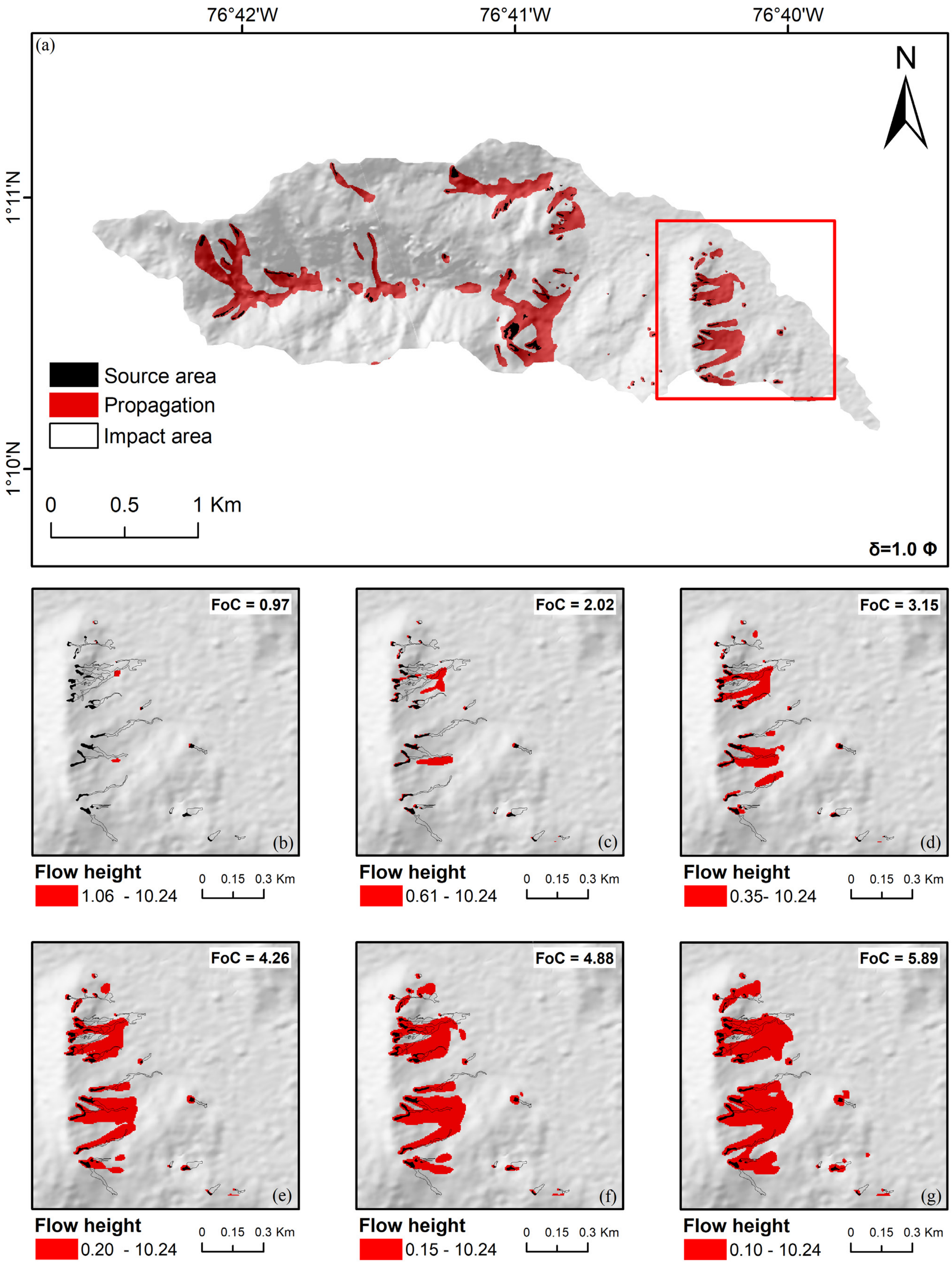

Figure 9. Modeling FoC and flow height (m) - Taruca creek

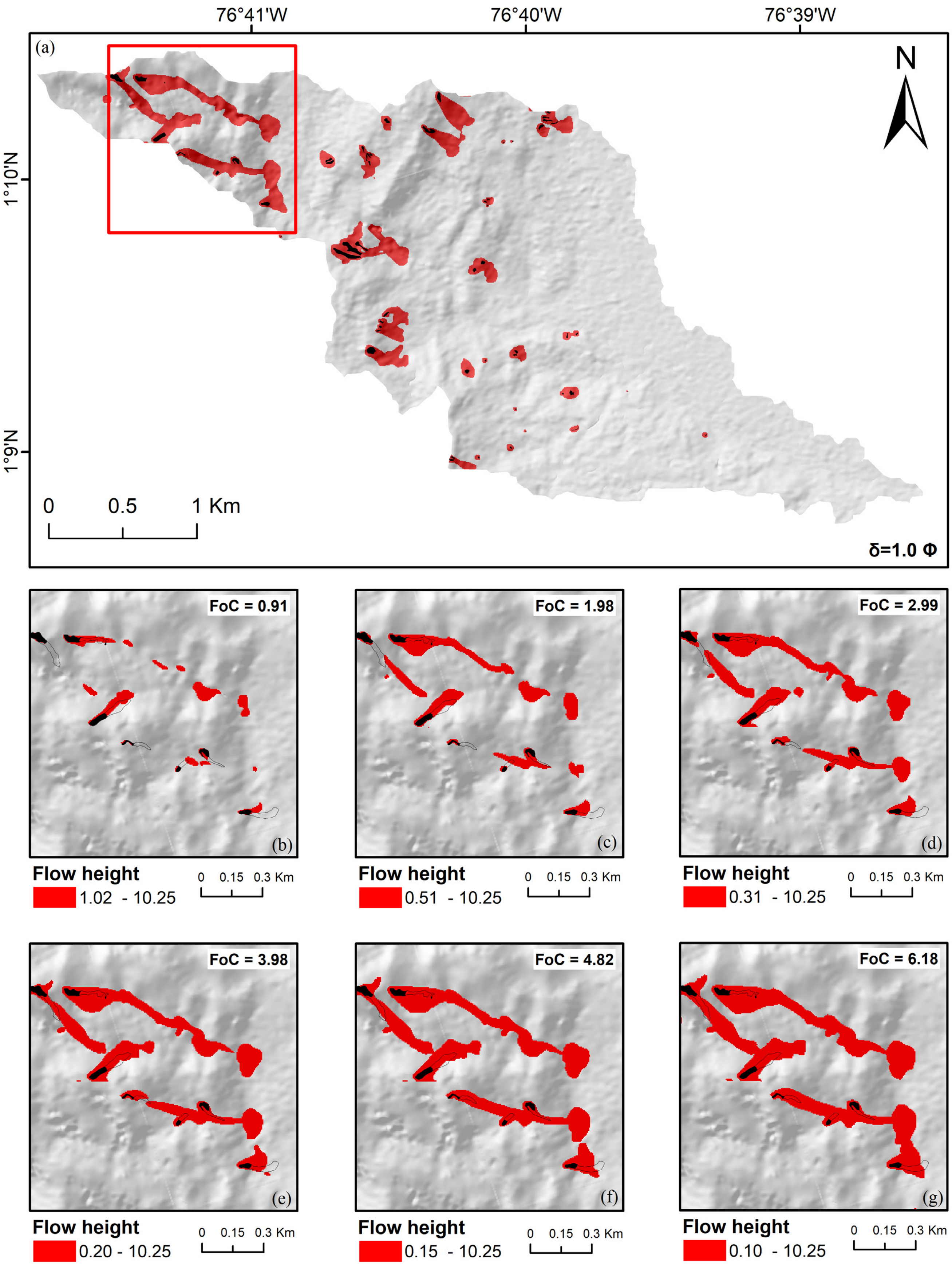

Figure 10. Modeling FoC and flow height (m) - Sangoyaco River

physical features, composition of material, and interaction with the terrain such as erosion and entrainment. Landslides are natural phenomena, therefore modeling them is challenging, with many elements affecting their downslope mobility. Estimate the hazard implies the assessment of the spatial probability of affectation and other variables, hence the importance of determining the possible areas affected, not only during the occurrence but also during the propagation. In runout process, the contact force between the moving mass and the terrain is represented by basal friction, which is one of the variables that determines the evolution of the nature of the phenomenon and thus the modeling. As a result, being a part of the erosion and entrainment processes. According to Hungr et al. (2014), the initial volume in many landslides is low in comparison to the volume from erosion and entrainment, particularly in channelized landslides. The availability of material to raise the volume of the mass as it moves is significant in humid tropical and high mountain environments like the research location. It has many low and medium-quality rocks, heavily weathered and fractured, mainly in an adjacent zone of the Mocoa - La Tebaida fault. in the transition between the eastern cordillera and the Amazonian foothills. Besides, in the 2016-2007 period, according to Qiu et al. (2007), vegetation cover changed considerably in the upper zone of the basin due to *El Niño*, leaving bare erodible soils exposed.

This study investigates the effect of basal friction variation on shallow landslide – debris flow propagation modeling. Low basal friction angles allow the mass to move at high velocity, resulting in longer travel distances; higher values result in lower velocities due to ground-material friction. Besides, the mass is constantly evolving due to the entrainment of the eroded material or deposition.

Based on the results obtained and presented above, none of the simulations ran got better validation metrics than the consideration of basal friction equal to internal friction. Although it better reflects the inventory of impacted areas, various basal friction produced comparable results, as shown in Figure 7 and Table 5. Also shows the second-best performance in terms of FoC~ 1 and F1- Score In the modeling of the Mulato River basin, the simulation with δ = 0.90 Ø produces an F1- Score of 0.345, values associated with a minimum flow height of 1.51 m. Therefore, it covers less area concerning the area affected and a height of 1.48 m of δ = 1.00 Ø. In the Taruca Creek basin, the second-best simulation was obtained with δ = 0.85 Ø, with a minimum flow height of 1.16 m and an F1-Score of 0.255; the height is 0.1 m higher than the obtained for δ = 1.00 Ø. The Sangoyaco River basin presents a slight variation between the heights associated with δ = 1.00 Ø and δ = 0.90 Ø. However, its F1-Score varies significantly, as does the FoC.

According to the results, FoC~ 2 has the highest F1-Score in the three basins. The minimum height from which the region affected for the simulated shallow landslide – debris flow propagations should be regarded is estimated from there, and it varies between 0.51 m and 0.61 m. In terms of modeling parameters for modeling shallow landslide – debris flow in r.avaflow, results suggest: (i) consider the basal friction equal to the internal friction of the material as the starting value; (ii) use minimum heights in the range of 0.51 m to 0.61 m to perform susceptibility zoning of the possible affected areas.

Table 5. Second-best performance in terms of FoC~ 1 and F1-Score

Basin	Basal friction	FoC	Flow height (m)	F1-Score
Mulato River	1.00 Ø	0.99	1.48	0.354
	0.90 Ø	1.00	1.51	0.345
Taruca Creek	1.00 Ø	0.97	1.06	0.278
	0.85 Ø	1.01	1.16	0.255
Sangoyaco River	1.00 Ø	0.91	1.03	0.310
	0.90 Ø	1.02	1.04	0.295

ACKNOWLEDGMENTS

Sincere thank the Geohazard Research Group for their support and assistance throughout the development of this work, as well as the project 'Evaluation of Hazard from Mass Movements and Debris Flows in Tropical and Mountainous Environments' at the National University of Colombia. Gratitude is also extended to the reviewers for their valuable contributions and to the editorial team for the careful handling of the manuscript.

REFERENCES

Instituto Nacional de Medicina legal y ciencia forenses (2017). INMLCF identifica 191 cuerpos en Mocoa; https://www.medicinalegal.gov.co.

Anderson, S. A. and Sitar, N. 1995. Analysis of Rainfall-Induced Debris Flows. Journal of Geotechnical Engineering 121(12): 544–552.

Aristizábal, E. and Sánchez, O. 2019. Spatial and temporal patterns and the socioeconomic impacts of landslides in the tropical and mountainous Colombian Andes. Disasters. 44(3): 596-618.

Campbell, R.H. 1974. Debris flows originating from soil slips during rainstorms in southern California. Journal of Engineering Geology and Hydrogeology 7(4): 339–349.

Cruden, D.M. and Varnes, D.J. 1996. Landslide types and processes. In: Turner, A.K. and Schuster, R.L. (eds.), Special Report 247. Landslides: Investigation and Mitigation, 36–75. Transportation and Road Research Board, National Academy of Science. Washington DC.

Dai, F.C., Lee, C.F. and Ngai, Y.Y. 2002. Landslide risk assessment and management: An overview. Engineering Geology 64(1): 65–87.

Dilley, M., Chen, R.S., Deichmann, U., Lener-Lam, A.L., Arnold, M., Agwe, J., Buys, P., Kjekstad, O., Lyon, B., Yetman, G., Lerner-Lam, A.L., Arnold, M., Agwe, J., Buys, P., Kjekstad, O., Lyon, B., and Yetman, G. 2005. Natural disaster hotspots: A global risk analysis. World Bank 34423, Hazard Management Unit. Disaster Risk Management Series No. 5, 132 p., Washington, DC.

Engelen, G. 1967. Landslides in the metamorphic northern border of the dolomites (north Italy). Engineering Geology 2(3): 135–147.

Fawcett, T. 2005. An introduction to ROC analysis. Pattern Recognition Letters 35(6): 299–309.

Froude, M.J. and Petley, D.N. 2018. Global fatal landslide occurrence from 2004 to 2016. Natural Hazards Earth System Sciences 18 (8): 2161–2181.

Gómez, D., García, E.F. and Aristizábal, E. 2023. Spatial and temporal landslide distributions using global and open landslide databases, Natural Hazards 117(1): 25-55.

Hungr, O., Corominas, J., and Eberhardt, E. 2005. Estimating landslide motion mechanism, travel distance and velocity. In: Hungr, O. Fell, R. Couture, R. and Eberhardt E. (eds.), Landslide risk management, 109–138. Francis & Taylor Group, London.

Hungr, O., Leroueil, S. and Picarelli, L. 2014. The Varnes classification of landslide types, an update. Landslides 11(2):167–194.

Kirschbaum, D. B., Adler, R., Hong, Y., Hill, S. and Lerner-Lam, A. 2009. A global landslide catalog for hazard applications: method, results, and limitations. Natural Hazards 52: 561-575.

Kjekstad, O. and Highland, L. 2009. Economic and Social Impacts of Landslides. Springer, Berlin, Heidelberg. In: Sassa, K. and Canuti, P. (eds.), Landslides–disaster risk reduction, Springer Berlin p 573-587. Heidelberg.

Medina Bello, E., Reyes Merchan, A.A., Castro, J.A., Sandoval Martínez, A., Torres, J. and Pérez Moreno, M. 2018. Observaciones de campo de la avenida torrencial del 12 de agosto de 2018 en el municipio de Mocoa - Putumayo. Technical Report. Servicio Geológico Colombiano. Bogotá.

Mergili, M., Fischer, J. T., Krenn, J. and Pudasaini, S.P. 2017. r.avaflow v1, an advanced open- source computational framework for the propagation and interaction of two-phase mass flows. Geoscientific Model Development 10(2): 53–569.

Moser, M. and Hohensinn, F. 1983. Geotechnical aspects of soil slips in Alpine regions. Engineering Geology 19(3): 185–211.

Núñez Tello, A. 2003. Reconocimiento geológico regional de la Planchas 411 La Cruz, 412 San Juan de Villalobos, 430 Mocoa, 431 Piamonte, 448 Monopamba, 449 Orito y 465 Churuyaco departamentos de Caquetá, Cauca, Huila, Nariño y Putumayo. Technical report, INSTITUTO DE INVESTIGACIÓN E INFORMACIÓN GEOCIENTÍFICA MINERO AMBIENTAL Y NUCLEAR INGEOMINAS, Bogotá, D. C.

Pastor, M., Blanc, T., Haddad, B., Petrone, S., Sanchez Morles, M., Drempetic, V., Issler, D., Crosta, G. B., Cascini, L., Sorbino, G. and Cuomo, S. 2014. Application of a SPH depth-integrated model to landslide run-out analysis. Landslides 11(5): 793–812.

Petley, D. 2012. Global patterns of loss of life from landslides. Geology 40(10): 927–930.

Poveda, G. 2004. La hidroclimatología de Colombia: una síntesis desde la escala interdecadal hasta la escala diurna. Revista de la Academia Colombiana de Ciencias, XXVIII(107): 201–222.

Prada-Sarmiento, L.F., Cabrera, M. ., Camacho, R., Estrada, N. and Ramos-Cañón, A.M. 2019. The Mocoa Event on March 31 (2017): analysis of a series of mass movements in a tropical environment of the Andean-Amazonian Piedmont. Landslides 16(12): 2459–2468.

Pudasaini, S.P. 2012. A general two-phase debris flow model. Journal Geophysical Research-Earth Surface 117(3): 1–28.

Pudasaini, S.P. and Krautblatter, M. 2021. The mechanics of landslide mobility with erosion. Nature Communications 12(1): 6793.

Pudasaini, S. P. and Mergili, M. 2019. A Multi-Phase Mass Flow Model. Journal of Geophysical Research-Earth Surface 124(12): 2920–2942.

Qiu, C., Xie, M. and Esaki, T. 2007. Application of GIS Technique in Three-Dimensional Slope Stability Analysis. Computational Mechanics 3(1): 703–712.

Quan Luna, B., Remaitre, A., van Asch, T.W., Malet, J.P. and van Westen, C.J. 2012. Analysis of debris flow behavior with a one-dimensional run-out model incorporating entrainment. Engineering Geology 128: 63–75.

RCN Radio 2017. Aumenta el número de personas muertas por avalancha en Mocoa.

Schuster, R. and Highland, L. 2003. Impact of landslides and innovative landslide-mitigation measures on the natural environment. Geologic Hazards Team, US Geological survey, 8(10): 1–46. Denver.

Schuster, R.L. and Highland, L. 2001. Socioeconomic Impacts of Landslides in the Western Hemisphere. US Geological Suvey, Open-File Report 01-276: 1–47.

SGC 2017a. Caracterización del movimiento en masa tipo flujo 31 de marzo 2017 en Mocoa- Putumayo. Technical report, Servicio Geológico Colombiano (SGC), Bogotá.

SGC 2017b. Sistema de Información de Movimientos en Masa - SIMMA. https://simma.sgc.gov.co

SGC 2017c. Zonificación de susceptibilidad y amenaza por movimientos en masa de las subcuencas de las quebradas Taruca, Taruquita, San antonio, El carmen y los ríos Mulato y Sangoyaco del municipio de Mocoa – Putumayo. Escala 1:25.000. Technical report, Servicio Geológico Colombiano (SGC), Putumayo.

SGC 2018a. Amenaza por movimientos en masa tipo flujo de las cuencas de las quebradas Taruga, Taruquita, San Antonio y El Carmen y los ríos Mulato y Sangoyaco, municipio de Mocoa, escala 1:5000. Technical report, Servicio Geológico Colombiano (SGC), Bogotá.

SGC 2018b. Evaluación de la amenaza por movimientos en masa en el área urbana, periurbana y de expansión del municipio de Mocoa

– Putumayo. Escala 1:5.000. Technical report, Servicio Geológico Colombiano (SGC), Mocoa.

Tayyebi, S.M., Pastor, M., Stickle, M.M., Yagüe, Á., Manzanal, D., Molinos, M. and Navas, P. 2022. SPH numerical modelling of landslide movements as coupled two-phase flows with a new solution for the interaction term. European Journal of Mechanics- B/Fluids, 96: 1–14.

Varnes, D.J. 1978. Slope Movement Types and Processes. Special Report 176: 11–33.

Varnes, D.J. 1984. Landslide hazard zonation: a review of principles and practice. UNESCO, Natural Hazard 3: 1-61, Paris.

Wang, Y., Hutter, K. and Pudasaini, S.P. 2004. The savage-hutter theory: A system of par tial differential equations for avalanche flows of snow, debris, and mud. ZAMM Zeitschrift fur Angewandte Mathematik und Mechanik 84(8): 507–527.